JOURNAL OF MAGNETIC RESONANCE **130,** 58–62 (1998)
ARTICLE NO. MN971256

SPARE: A Robust Method for Magnetic Resonance Imaging in Inhomogeneous Fields

D. J. O. McIntyre, F. Hennel,* and P. G. Morris†

*CRC Biomedical NMR Group, St. George's Hospital Medical School, Cranmer Terrace, Tooting, London SW17 0RE, United Kingdom; *FORENAP, Hospital Centre, 68250 Rouffach, France; and †Magnetic Resonance Centre, Department of Physics, University of Nottingham, Nottingham NG7 2RD, United Kingdom*

Received March 18, 1997; revised August 4, 1997

An imaging sequence based on a spin-echo train has been developed which is free from geometric distortions in the imaging plane due to main field inhomogeneity. Such inhomogeneities, and chemical shifts, cause only a displacement in the selected slice, which is minimized by the use of high gradient strengths and short radiofrequency pulses. Additionally, variations in the radiofrequency field strength cause variations in the image amplitude but cause no other artifacts. This allows the use of low-flip-angle refocusing pulses, reducing the power deposition to levels which are safe *in vivo* at high field strengths. The sequence was implemented on a Bruker whole-body 3T system. Example images from a perfluorocarbon phantom and a human head are presented. © 1998 Academic Press

Most magnetic resonance imaging sequences are sensitive to distortions due to main field inhomogeneities, which result from either sample susceptibility effects or imperfections in the magnet design. The distortions may be reduced either by increasing the read gradient strength at the expense of reducing the signal-to-noise of the image or by postprocessing, which is increasingly used to correct the distortion of echo-planar images along the blipped direction. In this work we describe a method which uses spin-echo trains to obtain images free from geometric distortion due to B_0 inhomogeneity, which is also insensitive to B_1 inhomogeneity, and demonstrate its use *in vivo.*

At the peak of a spin echo, all phase shifts due to field inhomogeneities and chemical shift offsets are refocused. It is therefore possible to generate an image by performing $n_x * n_y$ excitations, for each of which a single point is acquired at the top of a spin echo, following phase-encoding blips along both in-plane directions to move to the requisite point in *k*-space. However, this is slow. A single-point method based on FLASH has been published (*1*), which is faster owing to the shorter T_R used. For this sequence, the net phase shift due to inhomogeneity is identical for every point required, resulting in no overall distortion. However, it is sensitive to signal loss due to dephasing through the slice, and gives only T_2^* contrast.

It is possible to reduce the minimum time required to obtain an image by following the excitation with a CPMG train of hard π pulses which generate a series of spin echoes, and a number of sequences (*2–6*) which work in this way have been proposed. At the top of each spin echo one point is sampled (or a small number of points in the case of PACE (*5*)). Blips of gradient or a continuously oscillating sinusoidal gradient are used to obtain spatial resolution along one direction in-plane; in the other direction, phase encoding is used in the normal way. Figure 1 shows the sequence and *k*-space trajectory for one such accumulating-blip sequence.

While these sequences are capable of producing images free from geometric distortions due to main field inhomogeneities, streak artifacts are frequently observed at the edges or centers of the images. Some of these artifacts may be removed by phase cycling. To minimize the remaining artifacts, short, strong refocusing pulses are required, and the B_1 field must be extremely uniform across the sample. The power deposition of these sequences is therefore relatively high, limiting their use to low field strengths or applications such as microscopy or imaging of nonliving tissues where high-power pulses do not cause problems. PACE (*5*) uses fewer pulses, which reduces the power deposition and the artifacts due to pulse imperfections at the expense of reducing the range of field inhomogeneity that may be tolerated.

We have recently proposed (*7*) a new single-point CPMG train imaging method, SPARE (single-point acquisition with relaxation enhancement). This sequence uses slice-selective refocusing pulses and RARE (rapid acquisition with relaxation enhancement) (*8*) phase encoding, in which the phase-encoding gradients are fully rewound after each acquisition so that the net phase accumulation due to the gradients is zero. In such a sequence, all echoes, spin and stimulated, have the same phase encoding, which eliminates the streak artifacts observed with accumulating-blip techniques. This also allows refocusing pulses of flip angle less than 180° to be used, greatly reducing the power deposition. For the same reason, it is not greatly affected by B_1 inhomogeneity; reduction of the flip angle results in a reduction of image intensity

1090-7807/98 $25.00

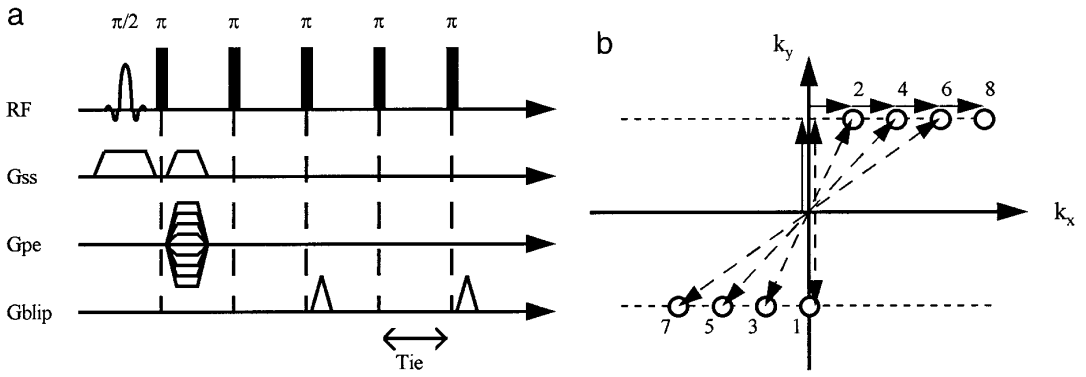

FIG. 1. (a) A pulse sequence for generating images undistorted by B_0 inhomogeneity. Magnetization excited by the initial pulse is repeatedly refocused by π pulses separated by a time T_{ie}. A single data point is sampled at the peak of each echo, where there is no phase shift due to B_0 offsets. Gradient blips interspersed between alternate RF pulses generate the complex *k*-space trajectory shown in (b) for the first eight points sampled in one echo train. The data are reordered prior to Fourier transformation.

but does not cause ghosting or geometrical distortion, as is the case with accumulating-blip techniques. The weighting of the echo amplitudes by the flip angle of the refocusing pulses is identical to that in RARE, which has been extensively analyzed. An analysis neglecting relaxation is given in (*9*) for a 90° excitation pulse followed by a train of refocusing pulses of flip angle α. This shows that a pseudo-steady state is reached after a few echoes where the echo amplitude is reduced by a factor $\sin(\alpha/2)$ relative to that obtained using 180° refocusing pulses; hence, the 30° pulse used for the brain images shown below would be expected to give 26% of the maximum attainable signal for 2.8% of the power deposition from the refocusing pulses. The effect of relaxation is considered in (*10*), where it is pointed out that, for 180° refocusing pulses, the decay of the echo amplitudes is determined only by T_2. For low-flip-angle refocusing pulses, the contributions of stimulated echoes make the echo amplitudes a complicated function of T_1, T_2, and flip angle. For $T_1 \gg T_2$, the signal loss to relaxation is significantly reduced at low refocusing flip angles, which effectively offsets part of the signal loss due to inefficient refocusing. The flip angle of 30° used for the brain images below was chosen to reduce the power deposition to safe levels and still gives images of good quality. The signal-to-noise ratio (SNR) of the brain SPARE images in Fig. 3 is half that obtained in the RARE brain images. SPARE and RARE images of a water phantom show identical SNR, due to the long T_2 of the water, the 180° refocusing pulses, and the identical filter width used for the two sequences.

The SPARE imaging sequence is shown in Fig. 2. It resembles the RARE imaging sequence (*8*) except that only a single point is acquired for each spin echo. A constant slice gradient G_{ss} is used to reduce the overhead for gradient switching times and to spoil FIDs from magnetization excited by the refocusing pulses. A full line of *k*-space (128 points) is acquired in each echo train. Any desired *k*-space trajectory may be followed by appropriate choice of the gradient blips; the images presented in this paper were obtained using the same trajectory followed by a normal 2D Fourier imaging experiment. G_{pe} is a standard phase-encode gradient blip except that it is rewound after each echo and then reapplied after the refocusing pulse. Its value is the same for each echo in a given train and is stepped for subsequent echo trains from $-G_{pe,max}$ to $+G_{pe,max}$. G_{blip} is a pseudo-read gradient, which is again rewound after each echo. Its value is incremented between each echo in a train from $-G_{blip,max}$ to $+G_{blip,max}$.

A disadvantage of SPARE is that it requires strong gradients, but for objects which have a T_2 of longer than 100 ms, a 2-mm-resolution image could be obtained with the 10 mT/m/1 ms gradients normally available on clinical imaging systems.

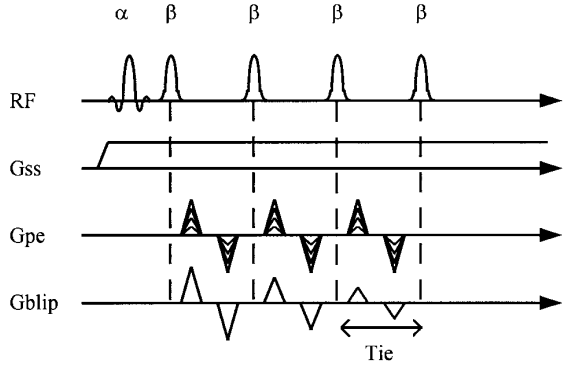

FIG. 2. The SPARE pulse sequence for imaging. The slice-select gradient G_{ss} is left on continuously throughout acquisition, crushing FIDs generated by the refocusing pulses. Magnetization excited by the initial α pulse is repeatedly refocused by the β pulses and a single data point is sampled at the peak of each echo. G_{pe} acts as a conventional phase-encoding gradient, except that the gradient is rewound after each data point is sampled and applied again after the refocusing RF pulse. G_{blip} acts as a pseudo-read gradient and is rewound and reapplied similarly to G_{pe}.

Since every point acquired is at the peak of an echo, there is no T_2^* weighting of the image. T_2 weighting may be adjusted by changing the order of acquisition of particular points in *k*-space, or by extending the echo train and not acquiring the earliest echoes. This represents a further advantage of SPARE over other single-point imaging techniques, as this may only be done with an accumulating-blip sequence by inserting a large negative blip in the place of one of the pseudo-read blips. This sacrifices the lower gradient requirements of these sequences and may affect the image quality by violating the CPMG conditions. However, for low-flip-angle refocusing pulses the SPARE image weighting will not be pure T_2.

T_1 weighting may be adjusted by changing the T_R within the limits permitted by power deposition; for the human studies presented in this paper, the minimum T_R was limited to 2 s. Splitting each echo train into two or more shorter trains allows the T_R to be further reduced.

It is difficult to calculate the exact effects of diffusion in the imaging gradients due to the large number of combinations of spin and stimulated echoes that must be considered, but straightforward to show that the effect is negligible in the worst case for the parameters used in the work described here. Only the slice-select gradient, which is switched on continuously and therefore has the largest effect, will be considered. The minimum diffusion weighting is obtained when all echoes are spin echoes, and is given by the standard formula

$$\frac{S}{S_0} = \exp\left(-\frac{2m}{3}\gamma^2 G^2 D\left(\frac{T_{ie}}{2}\right)^3\right), \qquad [1]$$

where D is the diffusion constant, taken for this estimate to be the constant for pure water $= 2 \times 10^{-9}$ m^2 s^{-1}; G is the slice-select gradient; T_{ie} is the interecho time; and m is the echo number; in the experiments performed, G was 14.75 mT/m, T_{ie} was 2.6 ms, and m had a maximum value of 128, giving a diffusion attenuation of less than 1%.

The maximum weighting is obtained when the magnetization is flipped up to the *z*-axis by the first refocusing pulse and restored to the *xy*-plane by the refocusing pulse before the final echo, and is given by the Stejskal–Tanner formula with $\delta = T_{ie}/2$ and $\Delta = T_{ie}(m-1)$:

$$\frac{S}{S_0} = \exp\left(-\gamma^2 G^2 \left(\frac{T_{ie}}{2}\right)^2 D\left((m-1)\left(\frac{T_{ie}}{2}\right) - \left(\frac{T_{ie}}{6}\right)\right)\right). \qquad [2]$$

This gives an attenuation which is slightly larger but remains less than 2%.

Susceptibility-induced gradients in human imaging are typically lower than the slice-select gradients used here, and so are unlikely to result in signal loss. In the extreme case of high-field plant microscopy, where gradients of up to 20 T m^{-1} can be induced in the immediate vicinity of intracellular air spaces (*11*), unreasonably short interecho times of around 50 μs would be required to reduce the losses to this level, and small signal voids will still be observed around the air spaces. Interecho times of around 1 ms and shorter trains of 8–16 echoes would, however, give images with much less loss to diffusion than conventional techniques.

The sequence was implemented on the Bruker MEDSPEC S300 3T whole-body imaging system at FORENAP. This system has hardware-based RF power deposition monitoring, allowing the sequence to be tested on humans safely. A quadrature birdcage head coil was used for ^{1}H experiments, and ^{19}F experiments were performed using a ^{19}F/^{1}H dual-tuned surface coil. Excitation was performed using a 1-ms 90° Gaussian pulse; 1-ms Gaussian refocusing pulses of flip angles from 30° to 180° were used. The T_R was 2000 ms to reduce the average power deposition. The blip gradient profiles were trapezoidal with a rise time of 300 μs and an overall duration of 700 μs, followed by a 100-μs stabilization delay prior to acquisition. The interecho time T_{ie} was 2.6 ms.

A head gradient insert capable of generating 28 mT/m was used for these images. The maximum gradient used for the experiments described here was 14.75 mT/m; 128^2 images were obtained with fields of view of 256 mm^2. Eight-echo or 16-echo RARE images were also obtained for comparison. Images were obtained with the objects well shimmed and with the field spoiled by offsetting the shims. No phase cycling was performed. The RARE filter width was 50 kHz; this bandwidth or smaller was used for the SPARE images. Theoretically, the bandwidth need only be as broad as the spread of frequencies in the object due to field inhomogeneities, to prevent parts of the image being cut off by the filter, and the SNR of the SPARE images is therefore less than optimal.

Experiments were performed on a water-filled sphere, the head of a normal volunteer, and a bottle of the perfluorocarbon FC40. RARE and SPARE human head images are presented in Fig. 3; (a) and (b) are RARE images, (c) and (d) are SPARE images, (a) and (c) are well shimmed, and (b) and (d) are spoiled by shim offset. For all images, the slice thickness was 3.3 mm. For the RARE images, eight echoes were acquired per excitation. Six-millisecond 180° Gaussian refocusing pulses were used, selecting a bandwidth of 330 Hz, and the slice selected in the unshimmed RARE image is therefore noticeably different from the slice selected in the shimmed RARE image. The unshimmed image is also distorted. The slice offset between the shimmed and unshimmed SPARE images is smaller, due to the 1-ms selective pulse of bandwidth 2000 Hz used for these. Again, there is no geometric distortion due to field offsets; additionally,

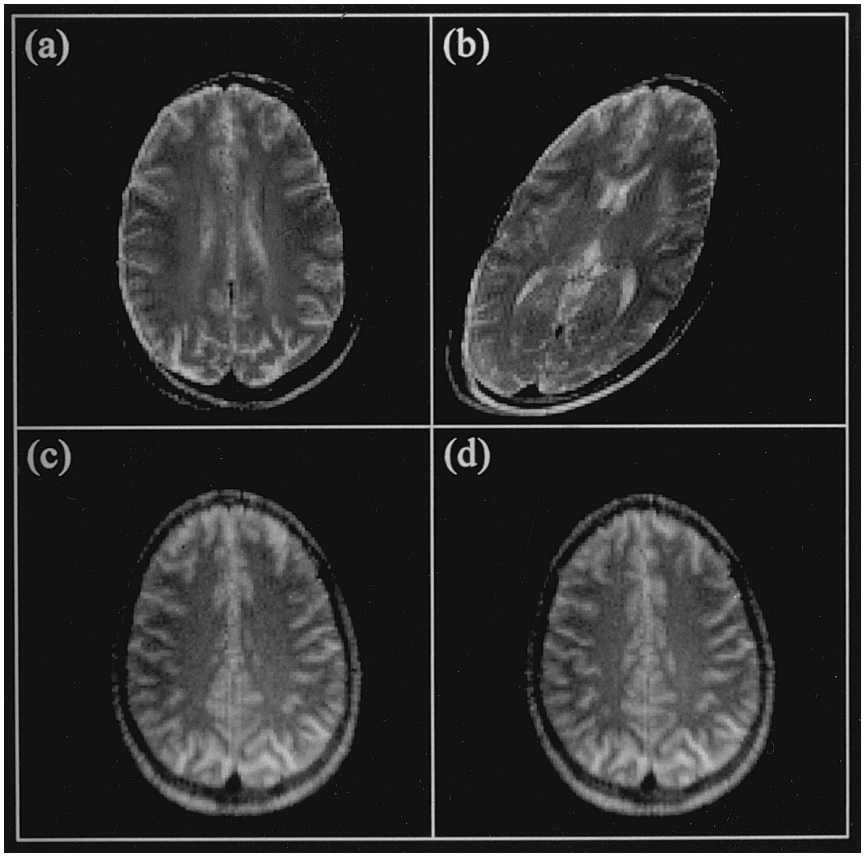

FIG. 3. (a) Shimmed and (b) mis-shimmed RARE images of the brain of a normal volunteer, obtained at 3 T. (c) Shimmed and (d) mis-shimmed SPARE images of the volunteer, distinguishable only by a slight misalignment of the selected slice. The use of low-flip-angle refocusing pulses minimizes RF heating but does not introduce geometric distortions or ghosting.

there is no chemical shift artifact and the fat image is correctly registered with the water image.

The chemical shift insensitivity is further demonstrated by the spectrum of Fig. 4 and the images in Fig. 5. Figure 4 is a spectrum obtained from a bottle of FC40 lying horizontally on top of a surface coil. Figure 5a is a ^{19}F gradient-echo image of the bottle with an image bandwidth of 20 kHz. Three images from the three resonances of FC40 may be seen. Figure 5b is a SPARE image of the same phantom with the same coil. In this image, the chemical shift artifact is eliminated. This image also demonstrates the insensitivity of the technique to B_1 inhomogeneity; the falloff of B_1 away from the coil is manifested only in a reduction of image intensity toward the top of the bottle. The intensity falls off by a factor of 5, where the gradient-echo image shows only a twofold reduction in intensity.

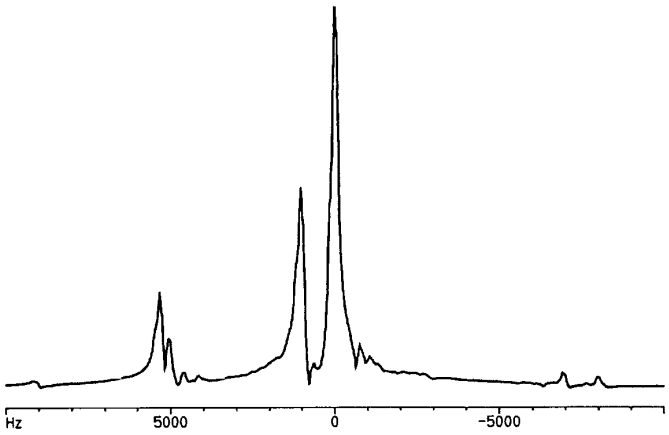

FIG. 4. ^{19}F spectrum obtained at 3 T from a bottle of the perfluorocarbon FC40 to demonstrate the wide chemical shift range of its resonances.

We have demonstrated a novel method for obtaining images free from in-plane artifacts due to main field inhomogeneities or chemical shifts. Slice displacement artifacts are minimized by the use of strong slice-select gradients and short RF pulses. It is also much more resistant to artifacts due to B_1 inhomogeneity than other similar sequences. This resistance is obtained at the expense of higher gradient requirements, although the peak amplitudes and switching times required of the gradients are no greater than those required for imaging techniques such as EPI. The power

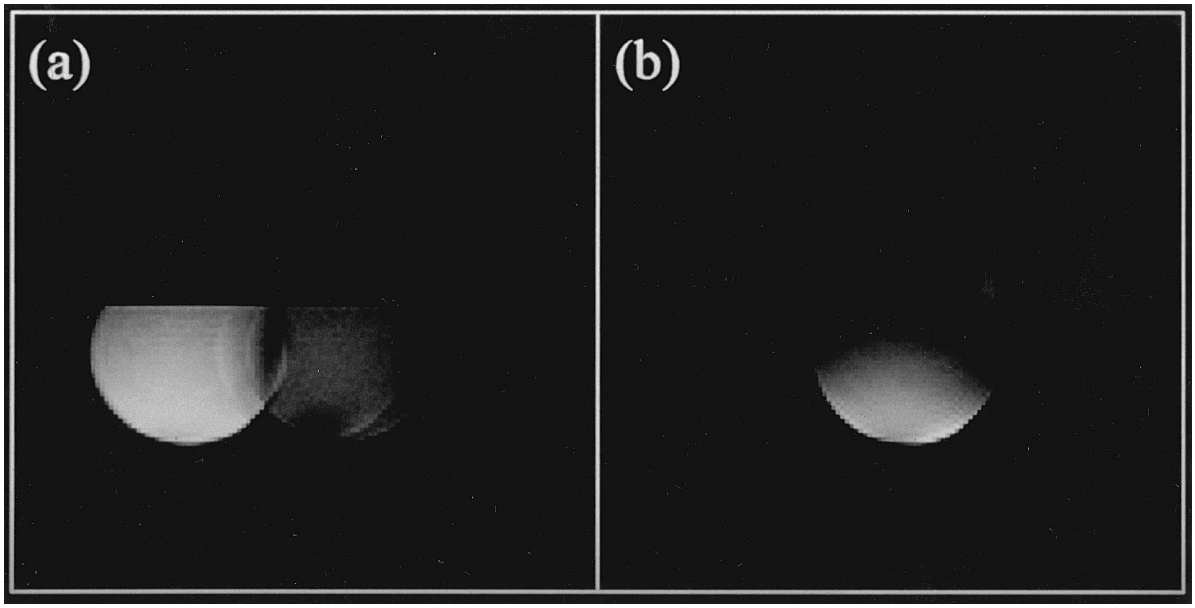

FIG. 5. (a) ^{19}F 2DFT image of a bottle of the perfluorocarbon FC40 lying on a surface coil. Multiple overlapping images result from the resonances of FC40. (b) SPARE image obtained with the same probe and sample as in (a), demonstrating the immunity to chemical shift and geometrical distortions due to B_1 inhomogeneity of this sequence.

deposition of the refocusing pulses is potentially quite high if 180° pulses are used; however, like RARE, the sequence still performs well when smaller flip angles are used, with relatively little degradation of the SNR. This sequence will have applications for imaging objects with high internal susceptibility variations and reasonably long T_2 values, and for imaging using magnets with inhomogeneous fields.

ACKNOWLEDGMENT

This work was partially supported by the Cancer Research Campaign (CRC), under Grant SP1971/0404.

REFERENCES

1. O. Heid and M. Deimling, *in* ''Proceedings, SMR, 1st Meeting,'' p. 684 (1995).
2. J. B. Miller and A. N. Garroway, *J. Magn. Reson.* **67,** 575 (1986).
3. P. Bendel, *IEEE Trans. Med. Imaging* **MI-4,** 114 (1985).
4. J. C. Sharp, R. W. Bowtell, and P. Mansfield, *Magn. Reson. Med.* **29,** 407 (1993).
5. J. K. Kim, D. B. Plewes, and R. M. Henkelman, *Magn. Reson. Med.* **33,** 497 (1995).
6. D. J. O. McIntyre, R. W. Bowtell, M.-J. Commandre, F. Hennel, P. Mansfield, and P. G. Morris, *in* ''The Bio–Clinical Interface'' (J.-P. Macher, M.-A. Crocq, and J.-F. Nedelec, Eds.), p. 349, John Libbey Eurotext, Paris (1995).
7. D. J. O. McIntyre, F. Hennel, and P. G. Morris, *in* ''Proceedings, ISMRM, 4th Scientific Meeting,'' p. 1537 (1996).
8. J. Hennig, A. Nauerth, and H. Friedburg, *Magn. Reson. Med.* **3,** 823 (1986).
9. J. Hennig, *J. Magn. Reson.* **78,** 397 (1988).
10. D. C. Alsop, *Magn. Reson. Med.* **37,** 176 (1997).
11. R. W. Bowtell, G. D. Brown, P. M. Glover, M. McJury, and P. Mansfield, *Philos. Trans. R. Soc. London A* **333,** 457 (1990).